Electronic Supplementary Material (ESI) for Inorganic Chemistry Frontiers.

Supporting Information For:

An eco-friendly approach by nonfluorous self-cleaning metal-organic framework composite and membrane for oil-water separation

*Abhijeet Rana, Subhrajyoti Ghosh, and Shyam Biswas**

Department of Chemistry, Indian Institute of Technology Guwahati, Guwahati, 781039 Assam, India.

* Corresponding author. Tel: 91-3612583309, Fax: 91-3612582349.

E-mail address: sbiswas@iitg.ac.in

Materials and General Methods:

All the reagents and solvents were purchased from commercial sources and used without further purification, except the 2-palmitamidoterephthalic acid (H_2BDC-NH-R) linker which was prepared according to the following procedure given below and the purity of the newly synthesized compound was examined by ^{1}H NMR, ^{13}C NMR, ATR-IR and mass spectrometric analysis (Fig. S1-S4). The melamine sponge and silk sheet were purchased from Amazon India. The Attenuated Total Reflectance Infrared (ATR-IR) spectra were recorded using PerkinElmer UATR Two at the ambient condition in the region 400-4000 cm^{-1}. The notations used for characterization of the bands are broad (br), strong (s), very strong (vs), medium (m), weak (w) and shoulder (sh). Thermogravimetric analysis (TGA) was carried out with a PerkinElmer TGA 4000 thermal analyzer in the temperature range of 30-700 °C under N_2 atmosphere at the rate of 4 °C min^{-1}. Powder X-ray diffraction (PXRD) instrument Rigaku Smartlab X-ray diffractometer (model: TTRAX III) with Cu-Kα radiation (λ = 1.54056 Å), 50 kV of operating voltage and 100 mA of operating current was used for the collection of all PXRD data. N_2 sorption isotherms were recorded by using Quantachrome Quadrasorb Evo volumetric gas adsorption equipment at −196 °C. Before the sorption analysis, the degassing of the compound was carried out at 120 °C under a high vacuum for 12 h. FE-SEM images were collected with a Zeiss (Sigma 300) scanning electron microscope. Gemini 500 was utilized for Energy Dispersive X-rays spectrometer (EDX) for elemental characterization. Pawley refinement was carried out using Materials Studio software. The DICVOL program incorporated within STOE's WinXPow software package was used to determine the lattice parameters. The contact angle measurements were performed by employing a Hol-marc HO-IOD-CAN-018 equipment at ambient temperature.

Synthesis of H_2BDC-NH-R:

The organic linker was synthesized using tetrahydrofuran (THF) as a solvent and pyridine as a base. 1 g (5.52 mmol) of 2-amino benzene-1,4-dicarboxylic acid and 1.75 mL (5.52 mmol) of palmitoyl chloride were taken in a round bottom flask containing 3.5 equivalents of pyridine. The mixture was refluxed for 24 h and then THF was evaporated. The resulting white powder was washed thoroughly with slightly acidic water to remove the excess pyridine. Further, it was washed with chloroform to remove any unreacted palmitoyl chloride to obtain the pure product. The ^{1}H NMR and ^{13C} NMR spectra are given below as Figure S1 and S2.

Measurement of Absorption Capacities for Various Oils by SH-UiO-66′@sponge Composite:

For the absorption of various heavy and light oils, fully dry pre-weighed (~250-300 mg) **SH-UiO-66′@sponge** composite was placed in various heavy oils ($CHCl_3$, CH_2Cl_2 and CCl_4) and light oils (hexane, ethyl acetate, petrol, diesel, crude oil, toluene, cyclohexane and kerosene). The composites were kept in oil for 1 min to reach absorption equilibrium and then removed and weighed. All the experiments were performed at room temperature. Absorption capacities for various oils were calculated using the following formula:

Absorption capacity (g/g) = $(W_f\text{-}W_i)/W_i$

where W_i is the initial weight of **SH-UiO-66′@sponge** and W_f is the weight of oil-absorbed **SH-UiO-66′@sponge**. Five measurements were performed for each oil sample and the average value was plotted.

Absorption-Based Separation of Oil and Water by SH-UiO-66′@sponge Composite:
A single piece of dry pre-weighed **SH-UiO-66′@sponge** composite (~250-300 mg) was placed in several oil/water combinations containing 3 mL of oil and 20 mL of water to separate the light oils (hexane, EtOAc, toluene, motor oil, gasoline and kerosene) from the surface of the water. For heavy oils (CH_2Cl_2, $CHCl_3$ and CCl_4), a piece of **SH-UiO-66′@sponge** composite was brought into contact with the sediment oil for the separation of heavy oils from the oil/water combination from the bottom of the water. For each case, the **SH-UiO-66′@sponge** composite selectively soaked the oils when it came into contact and the separated oil was recovered by physically squeezing the material. All the tests were performed at room temperature. Separation efficiency (%) for various oils was calculated using the following formula:

Separation efficiency (%) = V_f/V_i x 100%

where V_i was the amount of oil used (mL) and V_f was the absorbed volume of water (mL). Five measurements were performed for each oil sample and the average value was plotted.

Filtration-based separation of oils from the oil-water mixture by SH-UiO-66′@silk Membrane:
To separate different oils using the filtration-based method of separation, a round shaped piece of **SH-UiO-66′@silk** was bound with a round shaped solid circle and a mixture of different oils and water was allowed to pass through the membrane. The time needed for each step of the separation process was noted for each water-oil mixtures.

Separation efficiency (%) for various oil-water mixtures was calculated using the following formula:

Separation efficiency (%) = V_f/V_i x 100%

where V_i was the amount of oil used (mL) and V_f was the obtained volume of oil (mL) after the separation experiment.

The fluxes for the oil-water separation were determined using the formula: Flux = V/A × T (where V = volume of separated oil, A = area of the membrane and T = time required for the separation of oil from the oil-water mixture).

Separation of Emulsions Using SH-UiO-66′@silk Membrane:
All the water-in-oil emulsions were prepared (water/$CHCl_3$, water/toluene, water/ kerosene and water/gasoline) by sonicating the water-oil mixtures for 60 min. To make the emulsion stable, 50 µL of surfactant **(**Triton X-100) was added to the oil-water mixture before sonication. Then, 4 mL (3.5 mL of oils + 0.5 mL of water) of different water-in-oil emulsions were allowed to

pass through the **SH-UiO-66′@silk** membrane. The time required for all the separation processes were recorded.

Separation efficiency (%) for various water-in-oil emulsion were calculated using the following formula:

Separation efficiency (%) = V_f/V_i x 100%

where V_i was the amount of oil used (mL) for the preparation of the water in oil emulsion and V_f was the obtained volume of oil (mL) after the separation experiment.

The flux for various emulsions was calculated using a similar way (used in case of oil-water separation): Flux = V/A × T (where V = volume of separated oil, A = area of the membrane and T = time required for the separation of oil from water-in-oil emulsion).

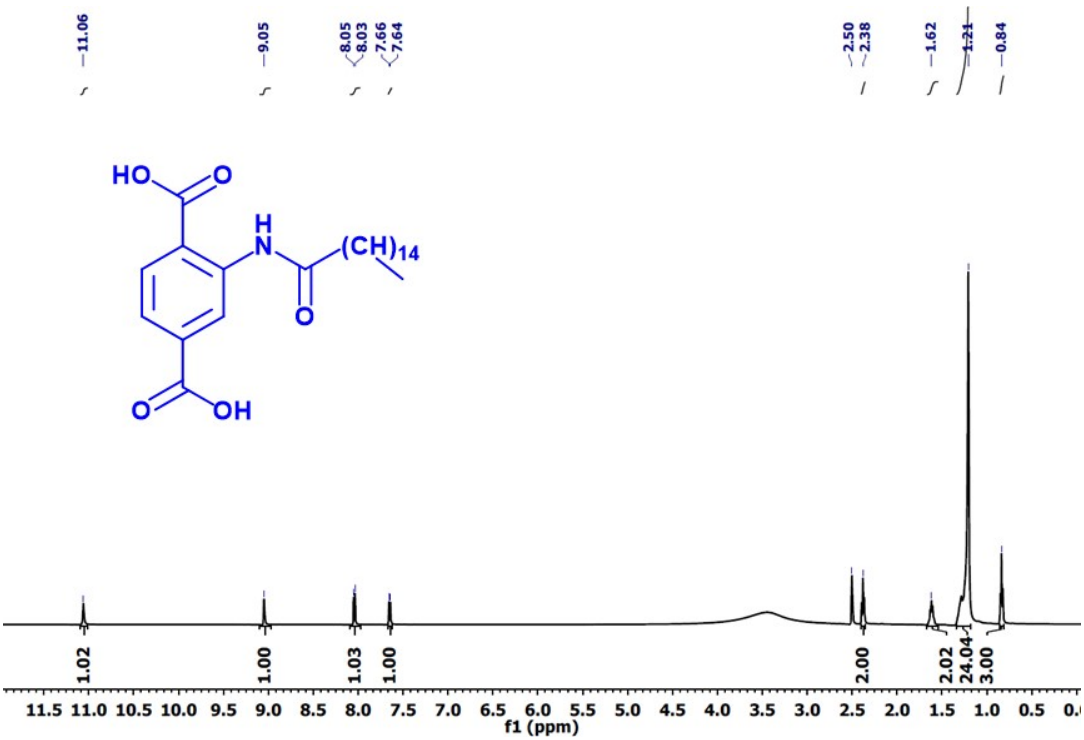

Fig. S1. ^{1}H NMR spectrum of H_2BDC-NH-R in DMSO-d_6.

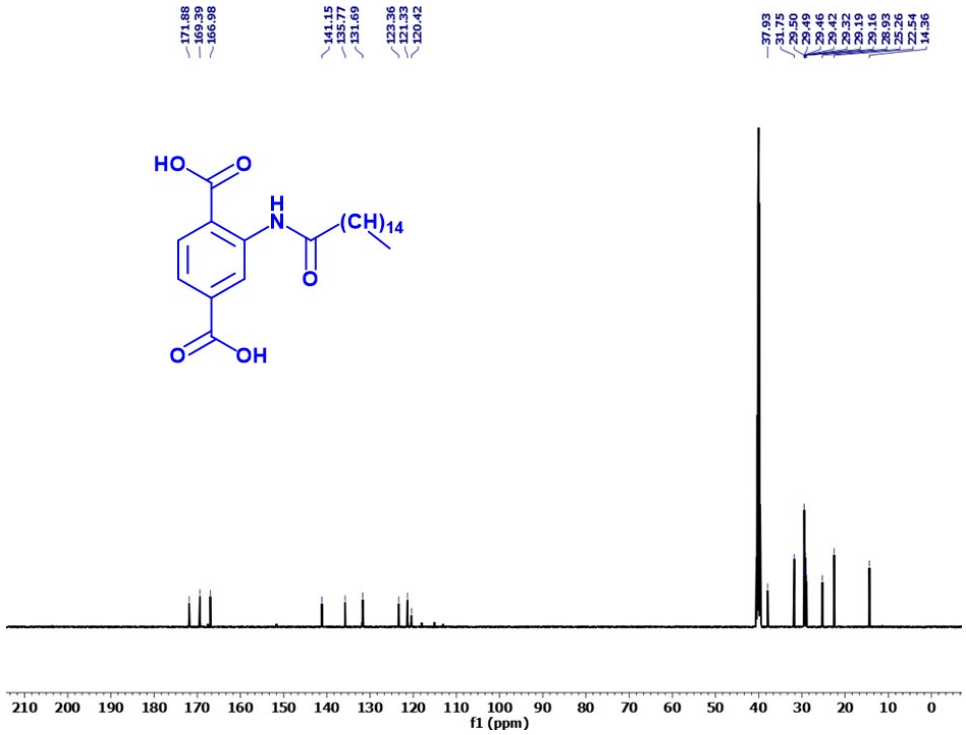

Fig. S2. ^{13}C NMR spectrum of H_2BDC-NH-R in DMSO-d_6.

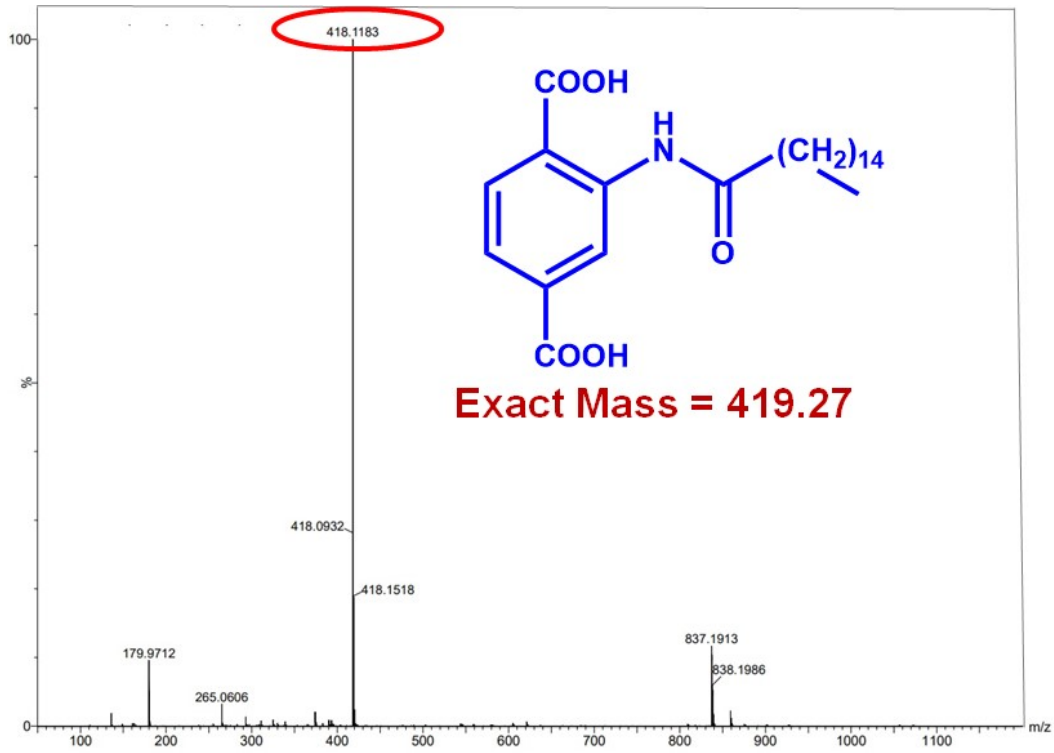

Fig. S3. ESI-MS spectrum of H_2BDC-NH-R measured in methanol. The spectrum shows m/z peak at 418.1183, which corresponds to $(M\text{-}H)^-$ ion (M = mass of H_2BDC-NH-R linker).

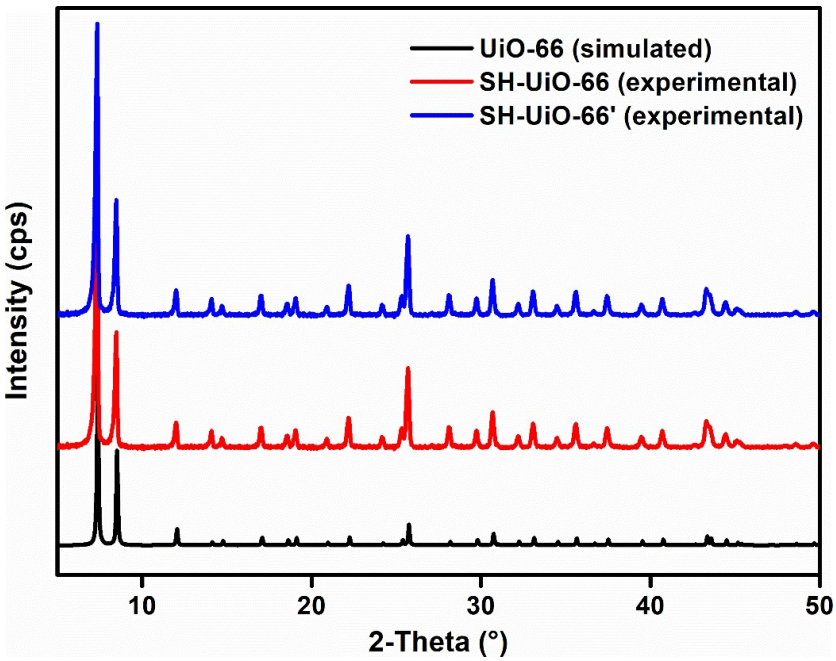

Fig. S4. PXRD patterns of (a) **Zr-UiO-66** (simulated), (b) **SH-UiO-66** and (c) **SH-UiO-66′**.

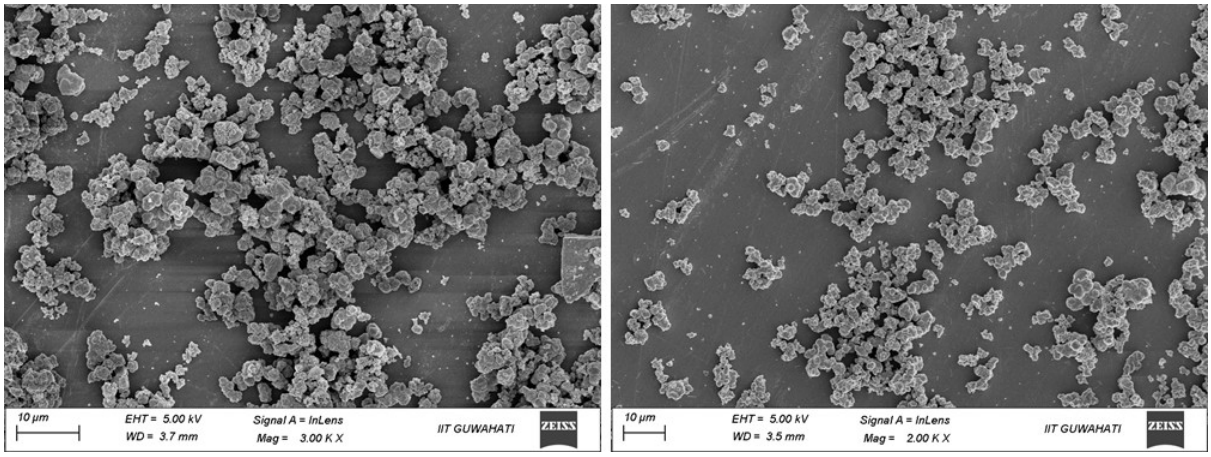

Fig. S5. FE-SEM images of **SH-UiO-66**.

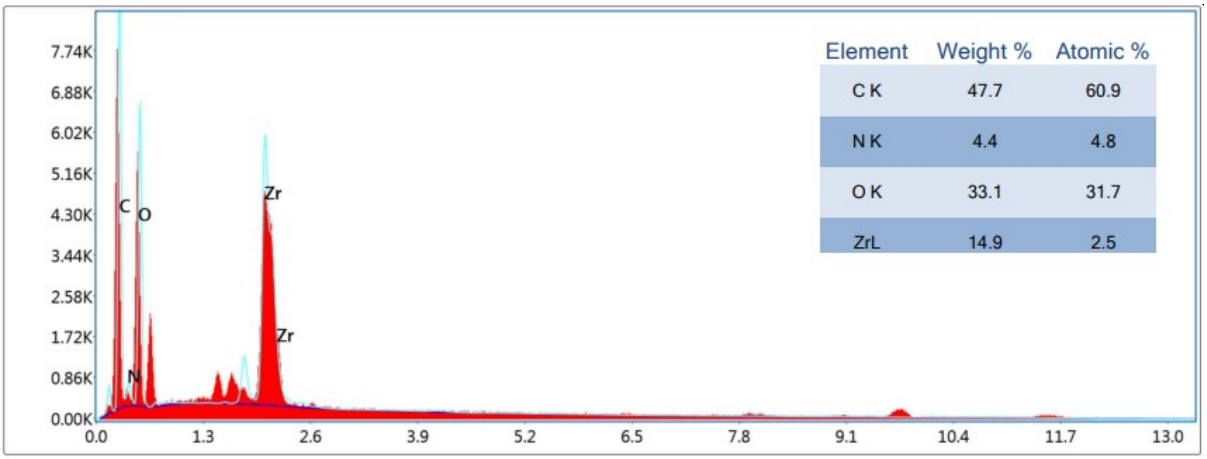

Fig. S6. EDX spectrum of **SH-UiO-66**.

Table S1. Unit cell parameters of **SH-UiO-66** obtained by indexing its PXRD data. The obtained values have been compared with parent UiO-66 MOF.

Compound Name	**SH-UiO-66**	UiO-66
Crystal System	cubic	cubic
a = b = c (Å)	20.753 (4)	20.790(3)
V (Å^3)	8938.3 (29)	8985.9(9)

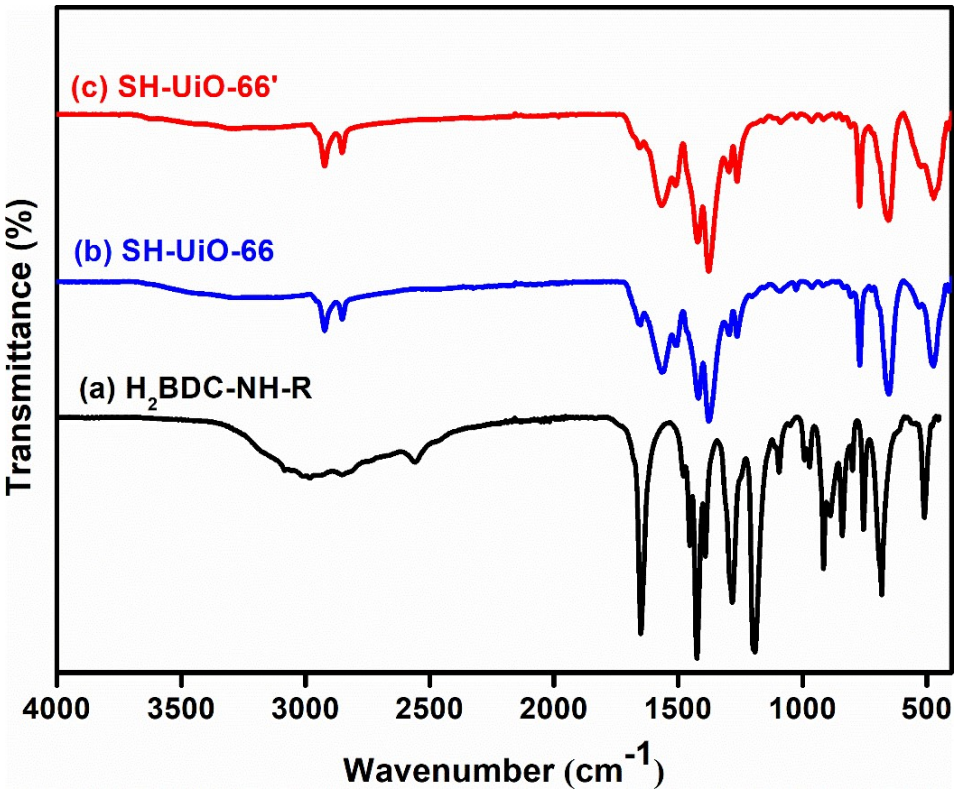

Fig. S7. ATR-IR spectra of (a) H_2BDC-NH-R linker, (b) **SH-UiO-66** and (c) **SH-UiO-66′.**

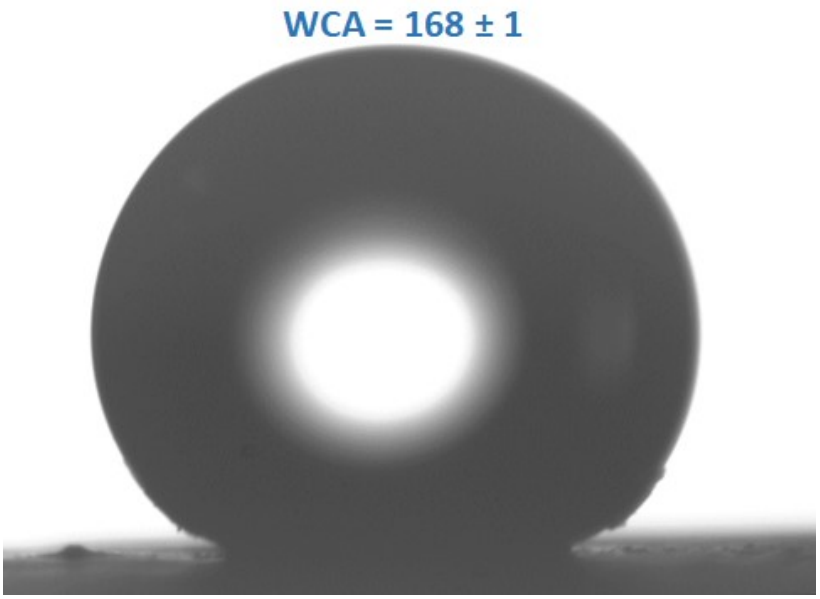

Fig. S8. Water contact angle (WCA) measurement image of **SH-UiO-66′**.

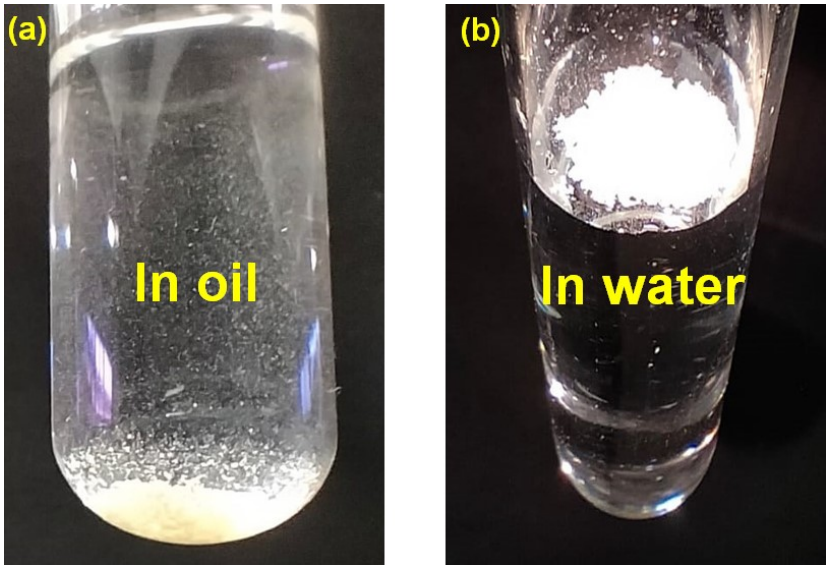

Fig. S9. Self-floating ability of **SH-UiO-66′** in water (a) and oil (hexane) (b).

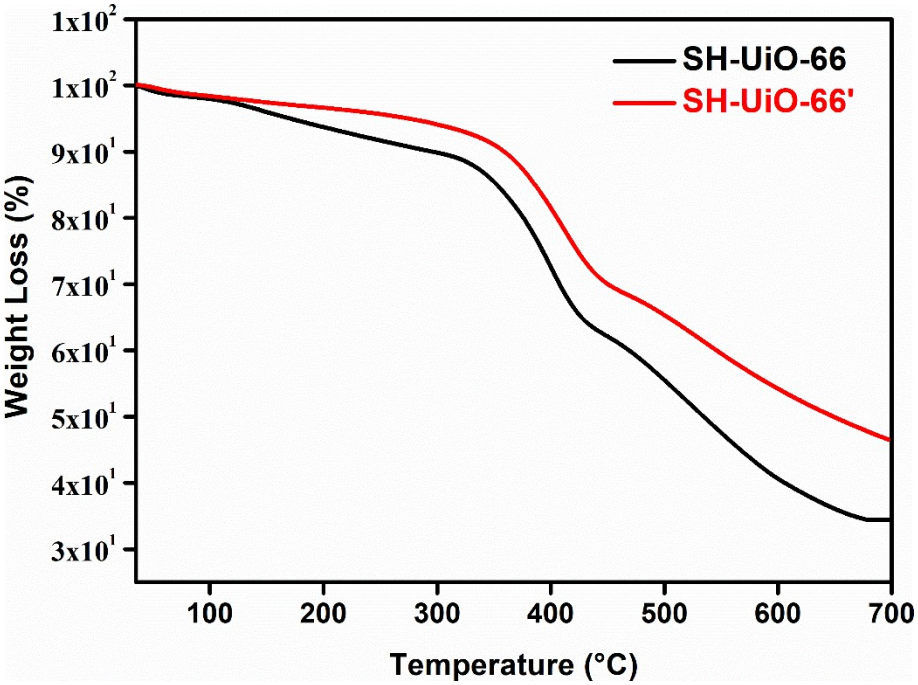

Fig. S10. TGA curves of as-synthesized **SH-UiO-66** (black) and activated **SH-UiO-66′** (red) recorded in N_2 atmosphere in temperature range of 30-700 °C at a heating rate of 4 °C min^{-1}.

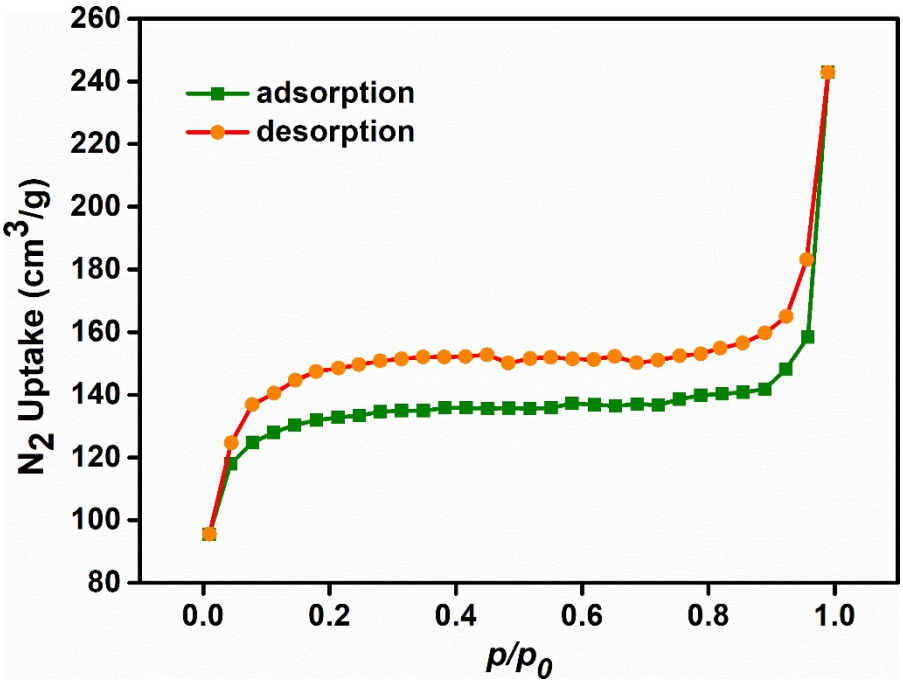

Fig. S11. Nitrogen adsorption and desorption isotherms of **SH-UiO-66′** recorded at –196 °C.

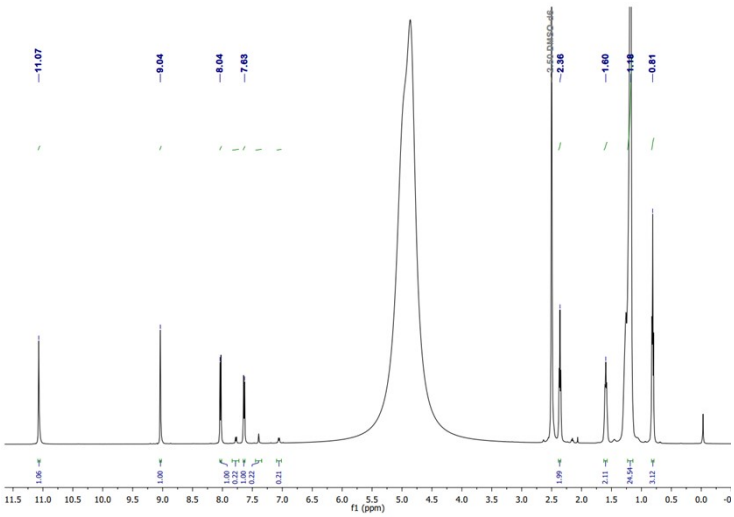

Fig. S12. The ^{1}H NMR spectra of SH-UiO-66 in DMSO-d_6 after digestion by HF.

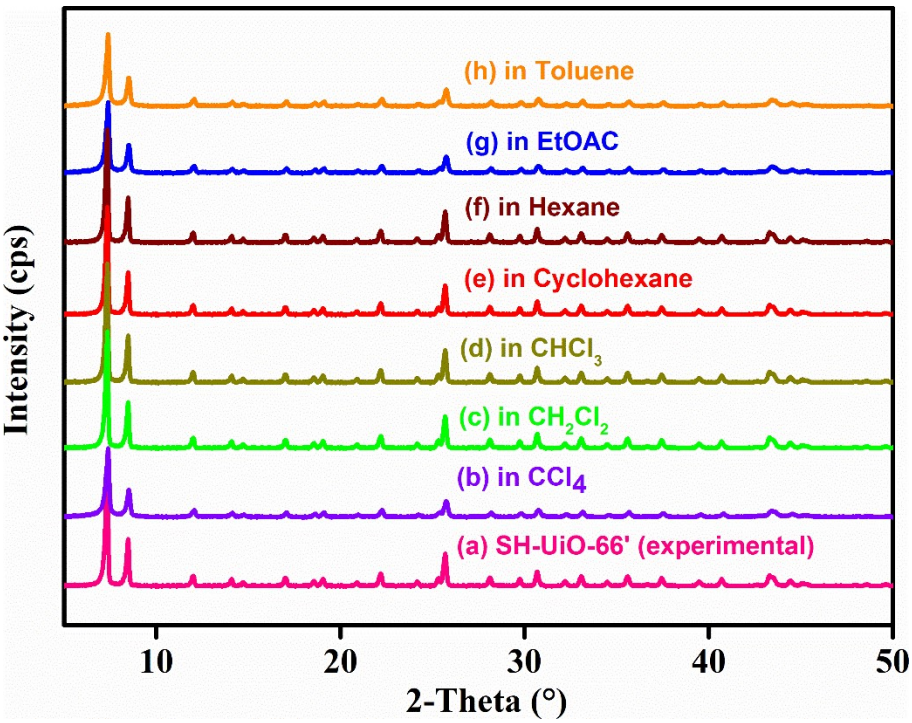

Fig. S13. PXRD patterns of (a) **SH-UiO-66′**, **SH-UiO-66′** after stirring in (b) CCl_4, (c) CH_2Cl_2, (d) $CHCl_3$, (e) cyclohexane, (f) hexane, (g) EtOAc and (h) toluene.

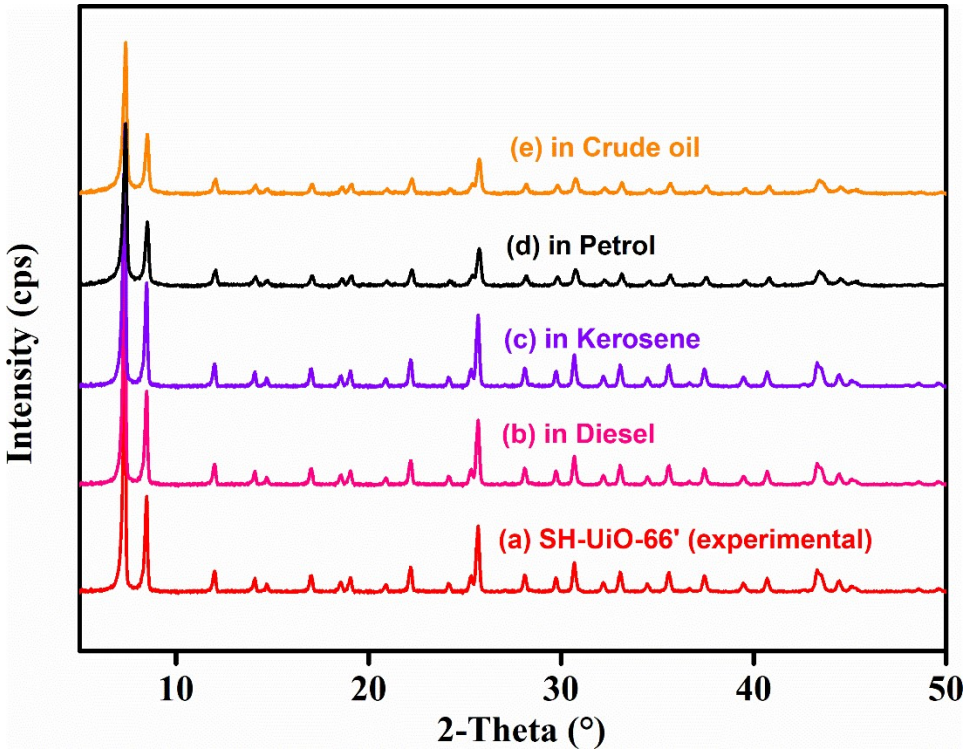

Fig. S14. PXRD patterns of (a) **SH-UiO-66′**, **SH-UiO-66′** after stirring in (b) diesel, (c) kerosene, (d) petrol and (g) crude oil for 24 h.

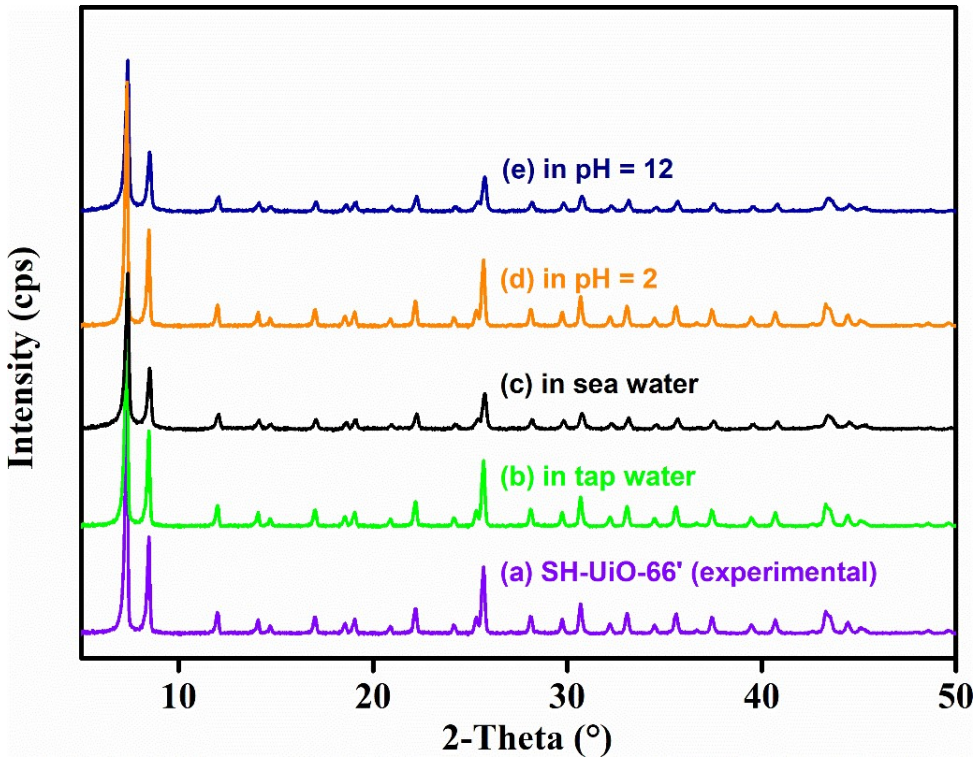

Fig. S15. PXRD patterns of (a) **SH-UiO-66′**, **SH-UiO-66′** after stirring in (b) tap water, (c) sea water, (d) pH = 2 and (e) pH = 12 for 24 h.

Table S2. Water Contact angle (WCA) of **SH-UiO-66′** after treatment with different types of water and oil specimens.

Liquids	Average WCA of **SH-UiO-66′** (°)
Fresh **SH-UiO-66′**	168 ± 1
CCl_4	169 ± 2
$CHCl_3$	167 ± 2
CH_2Cl_2	168 ± 1
Hexane	167 ± 1
Cyclohexane	168 ± 2
EtOAc	166 ± 2
Toluene	168 ± 3
kerosene	167 ± 1
Diesel	167 ± 2
Petrol	166 ± 1
Crude oil	165 ± 3
Tap water	168 ± 1
pH = 2	167 ± 1
pH = 12	165 ± 2
Sea water	166 ± 1

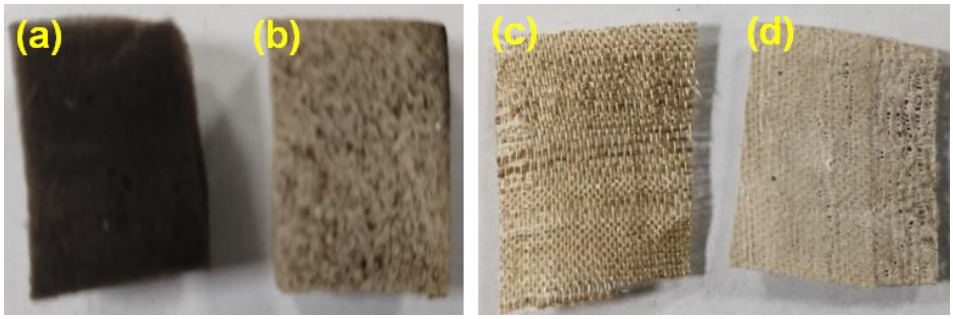

Fig. S16. Digital images of (a) polymer-coated sponge, (b) **SH-UiO-66′@sponge** composite, (c) polymer-coated silk membrane and (d) **SH-UiO-66′@silk** membrane.

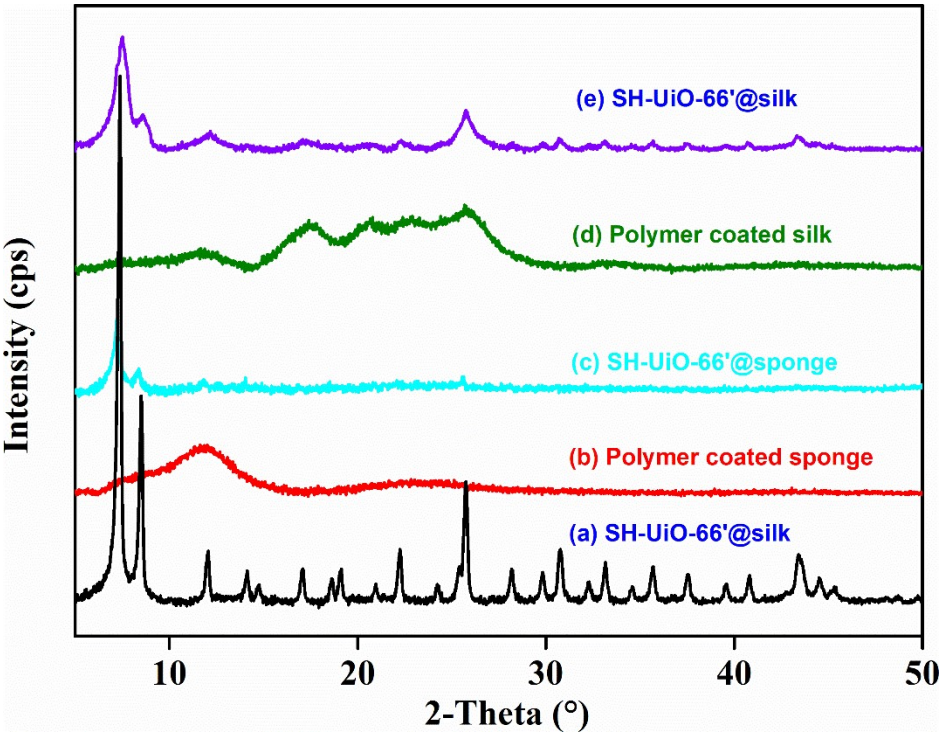

Fig. S17. PXRD patterns of (a) activated **SH-UiO-66′** (b) **SH-UiO-66′** polymer-coated sponge (c) **SH-UiO-66′@sponge** composite and (d) polymer-coated silk membrane and (e) **SH-UiO-66′@silk** membrane.

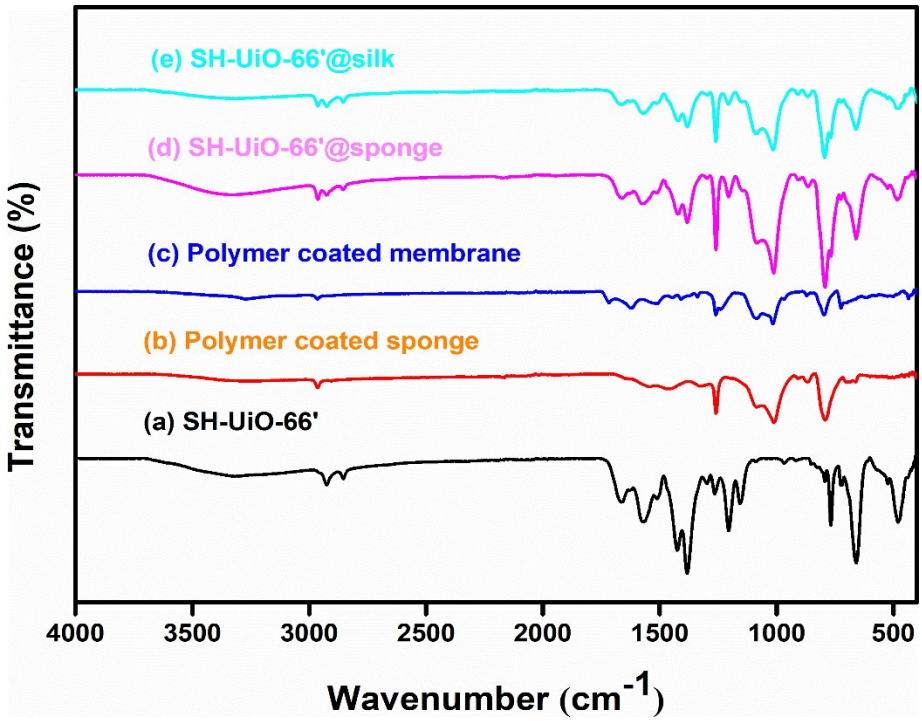

Fig. S18. ATR-IR spectra of (a) activated **SH-UiO-66′**, (b) polymer-coated sponge, (c) polymer-coated membrane, (d) **SH-UiO-66′@sponge** composite and (e) **SH-UiO-66′@silk** membrane.

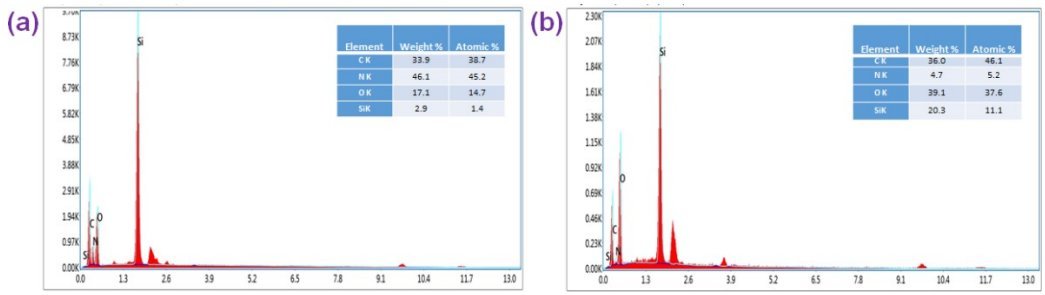

Fig. S19. EDX spectrum of (a) melamine sponge and (b) sheet of silk.

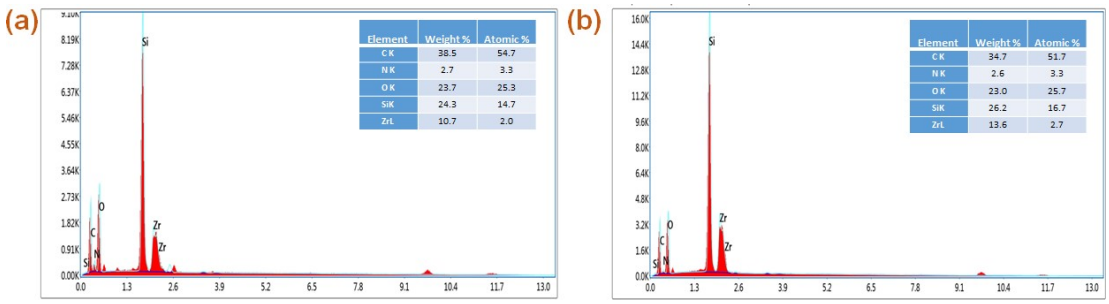

Fig. S20. EDX spectrum of (a) **SH-UiO-66′@sponge** composite and (b) **SH-UiO-66′@silk** membrane.

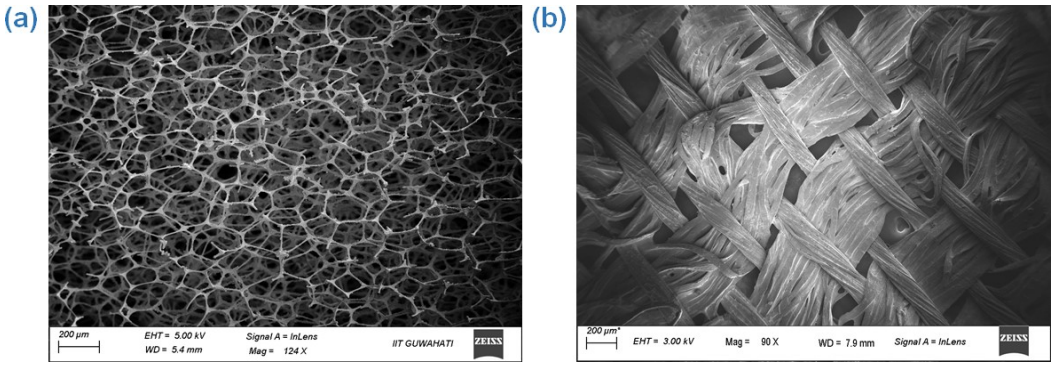

Fig. S21. High-resolution FE-SEM images of (a) melamine sponge and (b) silk sheet.

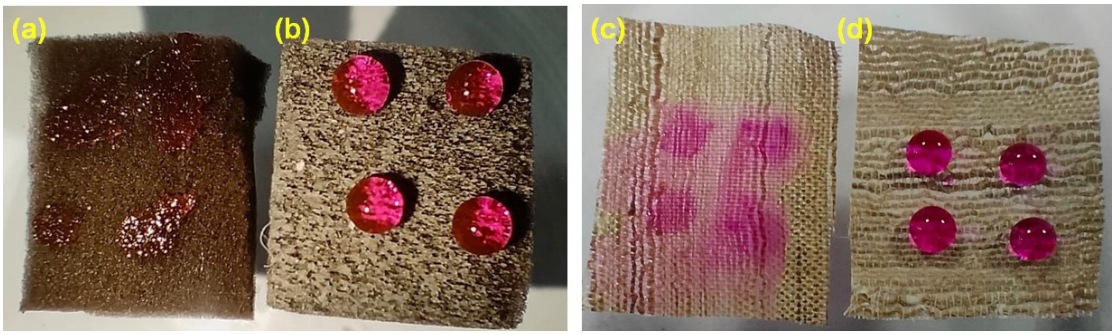

Fig. S22. Digital image of beaded water droplets on the surface of (a) polymer-coated sponge, (b) **SH-UiO-66′@sponge** composite, (c) polymer-coated membrane and (c) **SH-UiO-66′@silk** membrane.

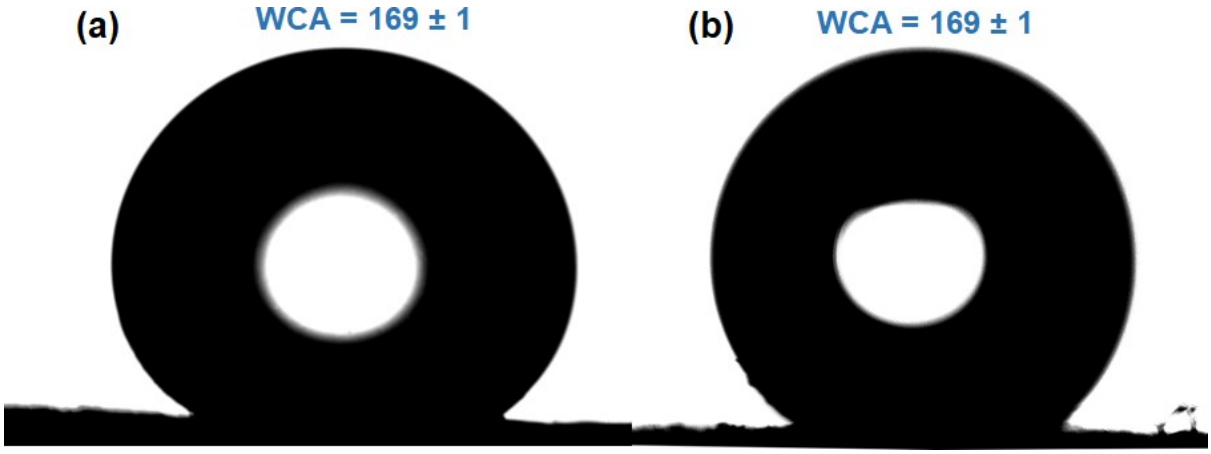

Fig. S23. The contact angle image of beaded water droplets on the surface of (a) **SH-UiO-66′**, (b) **SH-UiO-66′@sponge** composite and (b) **SH-UiO-66′@silk** membrane.

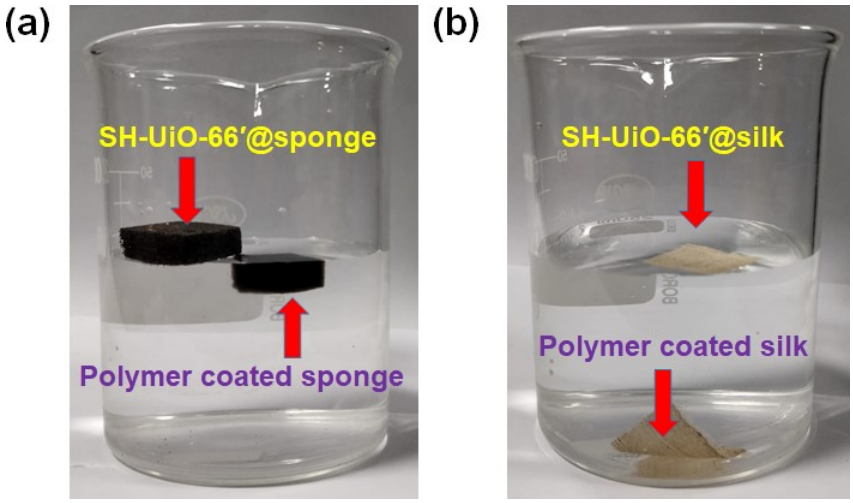

Fig. S24. (a) Digital images of floating **SH-UiO-66′@sponge** composite and immersion of polymer-coated melamine sponge. (b) Digital images of floating **SH-UiO-66′@silk** membrane on water and immersion of polymer-coated silk fabric in water.

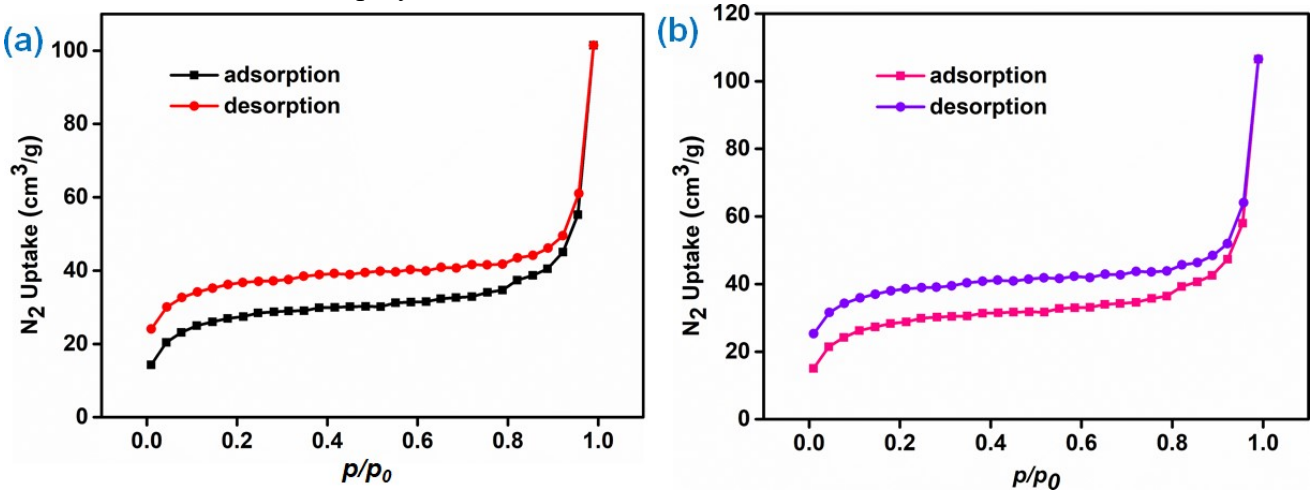

Fig. S25. Nitrogen adsorption and desorption isotherms of (a) **SH-UiO-66′ sponge** and (b) **SH-UiO-66′silk** recorded at –196 °C.

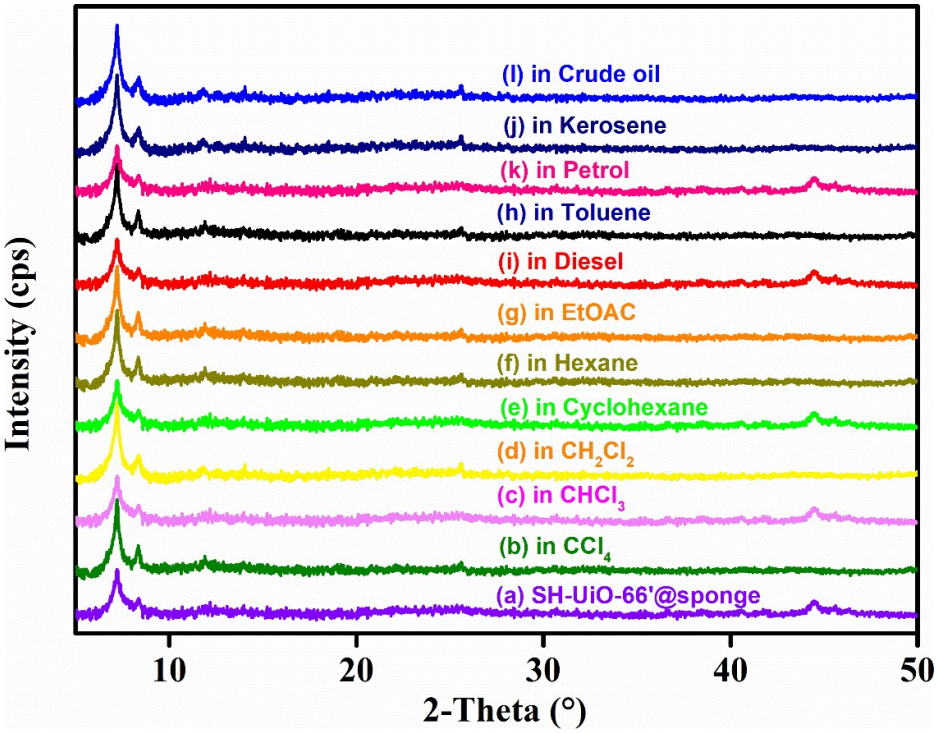

Fig. S26. PXRD patterns of (a) **SH-UiO-66′@sponge** composite after treatment with different types of oil specimens.

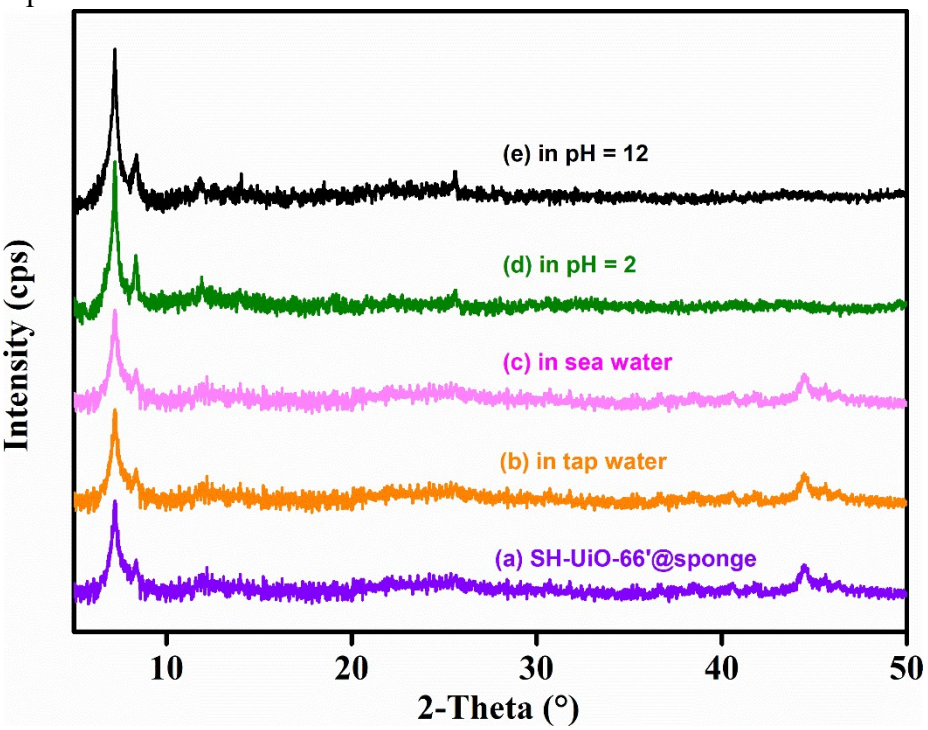

Fig. S27. PXRD patterns of (a) **SH-UiO-66′@sponge** composite after treatment with different types of water specimens.

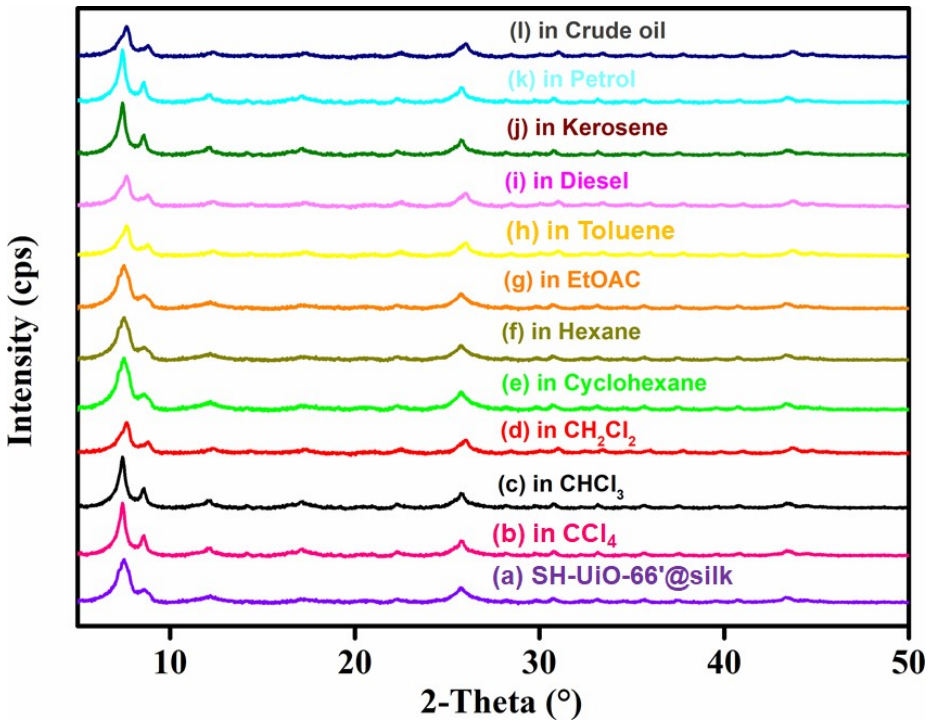

Fig. S28. PXRD patterns of (a) **SH-UiO-66′@silk** membrane after treatment with different types of oil specimens.

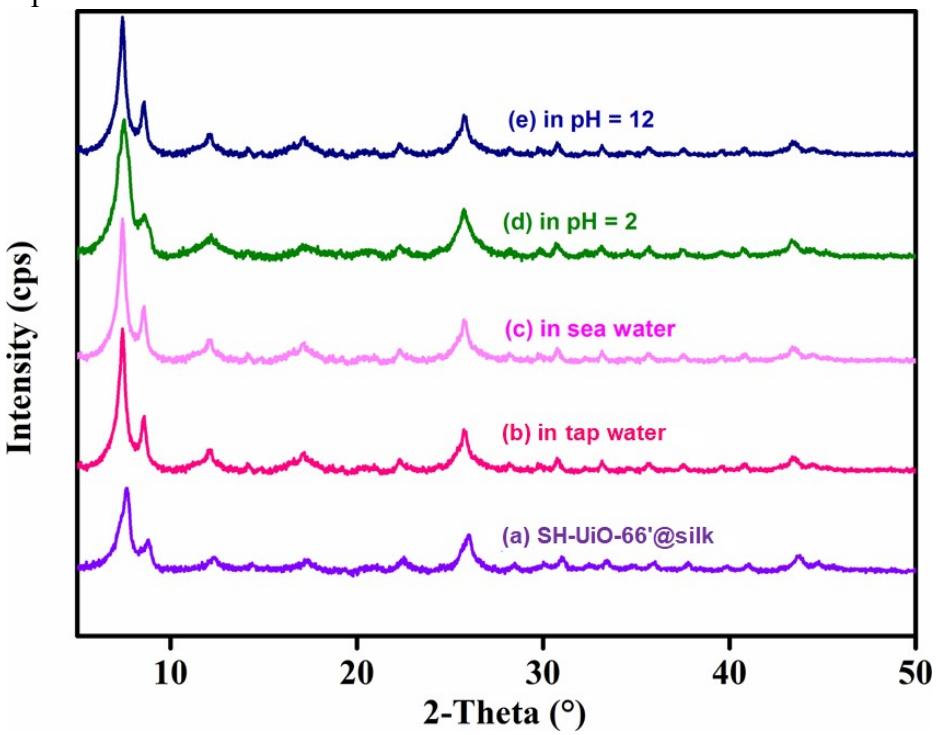

Fig. S29. PXRD patterns of (a) **SH-UiO-66′@silk** membrane after treatment with different types of water specimens.

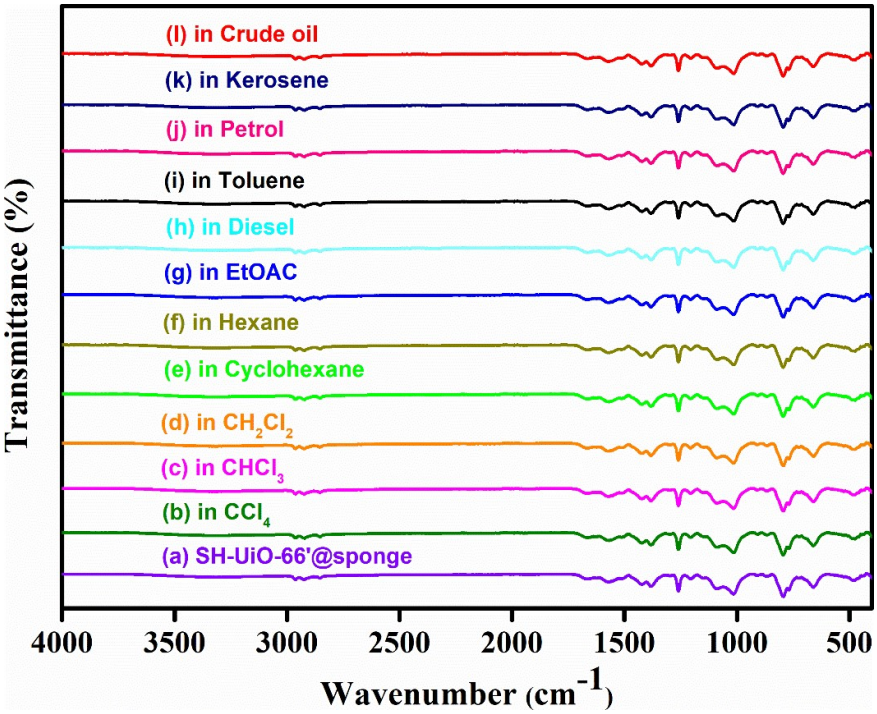

Fig. S30. ATR-IR spectra of (a) **SH-UiO-66′@sponge** composite after treatment with different types of oil specimens.

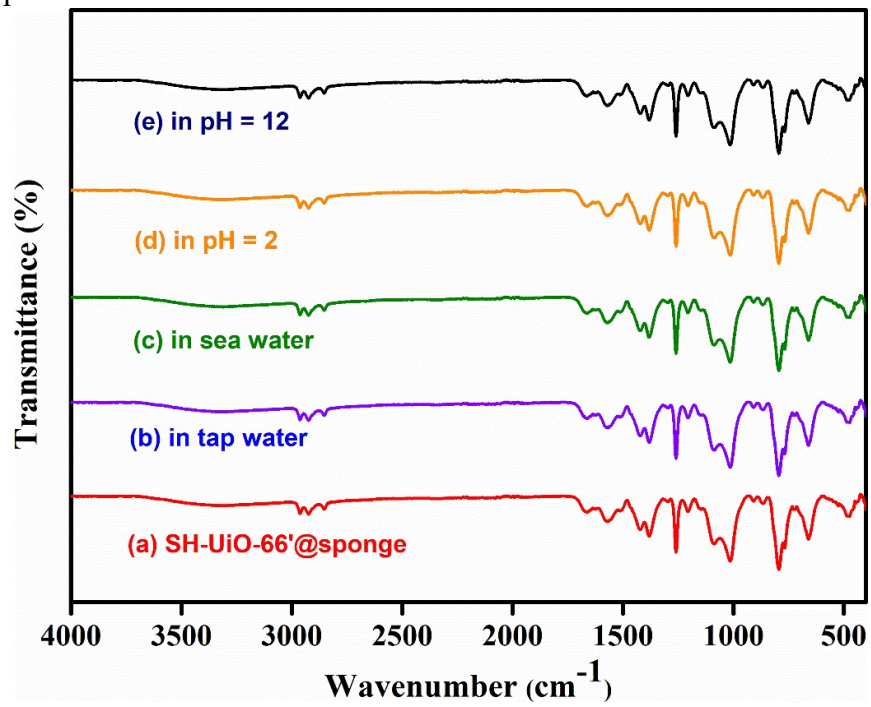

Fig. S31. ATR-IR spectra of (a) **SH-UiO-66′@sponge** composite after treatment with different types of water specimens.

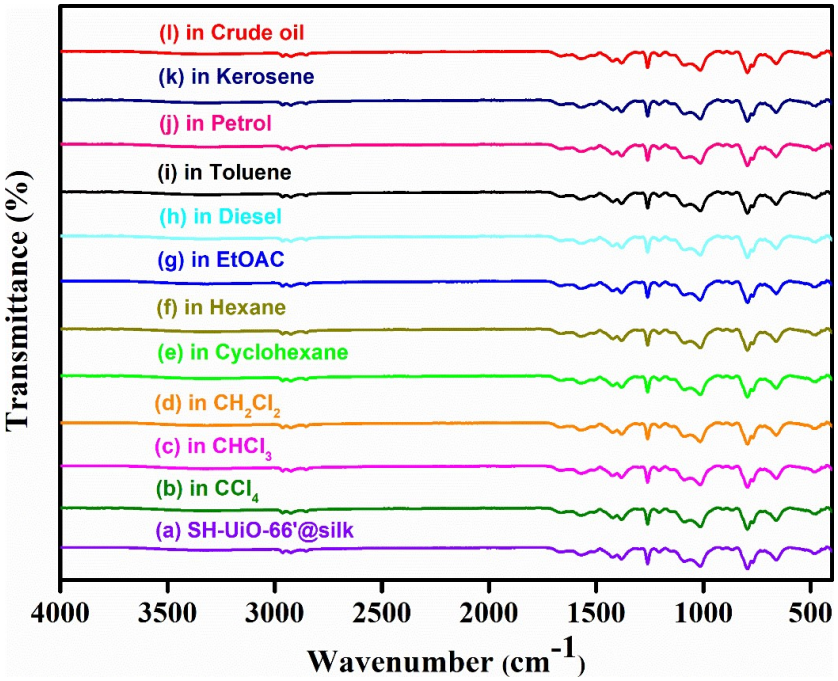

Fig. S32. ATR-IR spectra of (a) **SH-UiO-66′@silk** composite after treatment with different types of oil specimens.

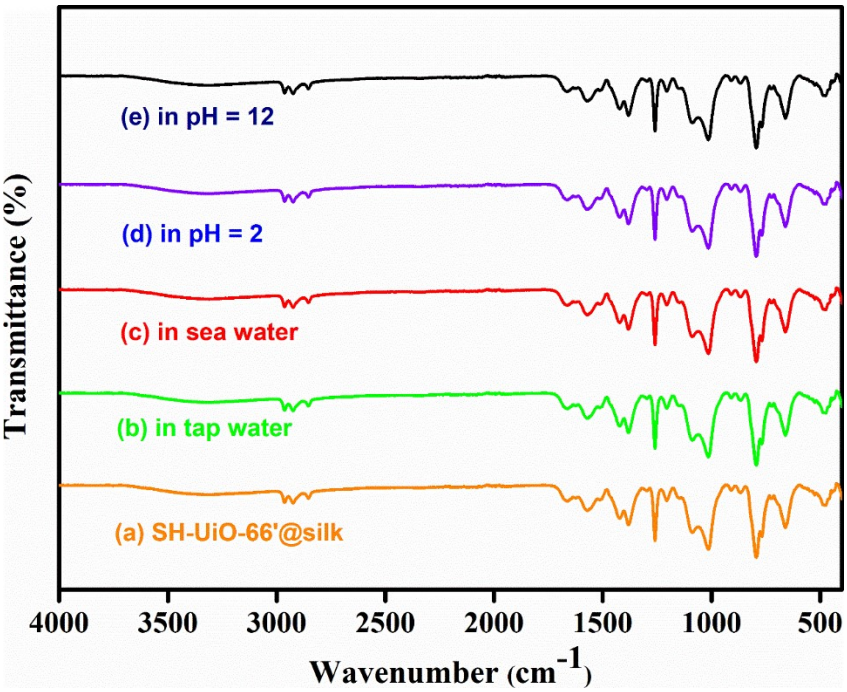

Fig. S33. ATR-IR spectra of (a) **SH-UiO-66′@silk** composite after treatment with different types of water specimens.

Table S3. Water Contact angle (WCA) of **SH-UiO-66′@sponge and SH-UiO-66′@silk** after treatment with different types of water and oil specimens.

Liquids	Average WCA of **SH-UiO-66′@sponge** and **SH-UiO-66′@silk** (°) after stirring in different liquids
Fresh **SH-UiO-66′@sponge** and **SH-UiO-66′@silk** (°)	169 ± 1 and 169 ± 1
CCl_4	167 ± 1 and 168 ± 2
$CHCl_3$	169 ± 2 and 168 ± 1
CH_2Cl_2	167 ± 2 and 168 ± 1
Hexane	167 ± 2 and 167 ± 2
Cyclohexane	166 ± 2 and 168 ± 1
EtOAc	167 ± 1 and 168 ± 2
Toluene	169 ± 2 and 167 ± 2
kerosene	167 ± 2 and 167 ± 1
Diesel	167 ± 2 and 168 ± 1
Petrol	167 ± 1 and 169 ± 2
Crude oil	169 ± 2 and 167 ± 2
Tap water	169 ± 2

	and 169 ± 1
pH = 2	166 ± 1 and 167 ± 2
pH = 12	166 ± 2 and 165 ± 3
Sea water	165 ± 2 and 167 ± 2

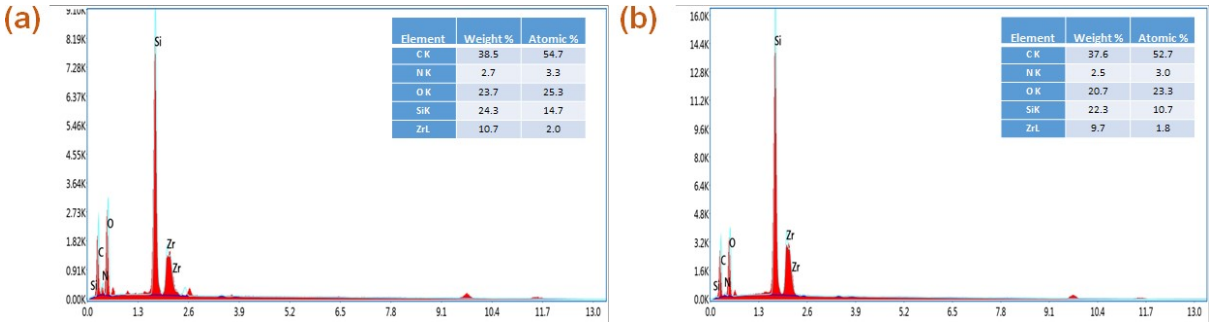

Fig. S34. EDX spectrum of (a) **SH-UiO-66′@sponge** composite and (b) **SH-UiO-66′@silk** after 70th and 60th cycle of oil-water separation experiments, respectively.

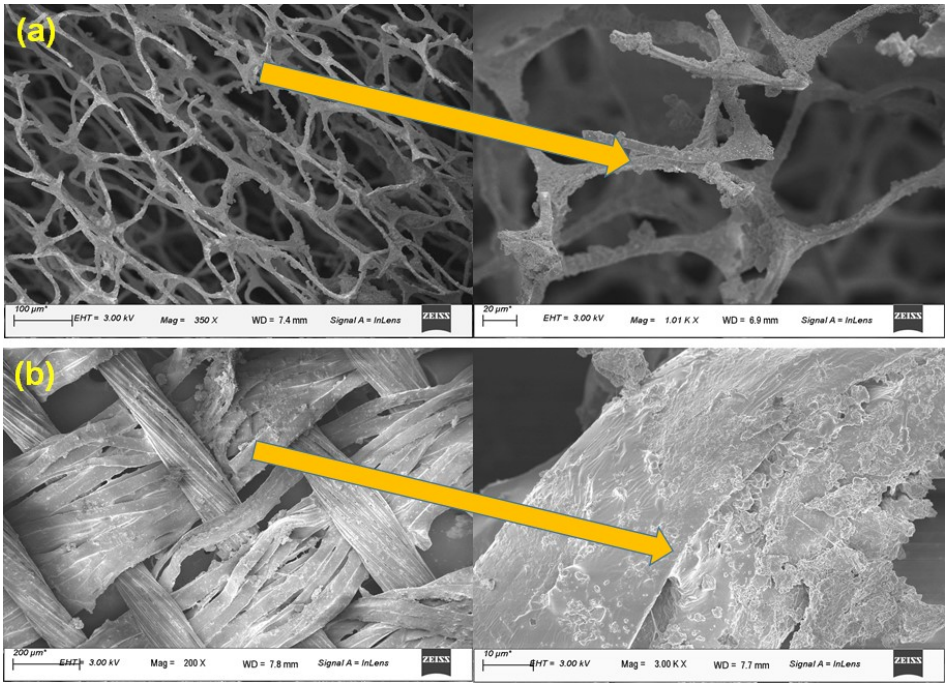

Fig. S35. High-resolution FE-SEM images of (a) **SH-UiO-66′@sponge** composite and (b) **SH-UiO-66′@silk** after 70th and 60th cycle of oil-water separation experiments, respectively.

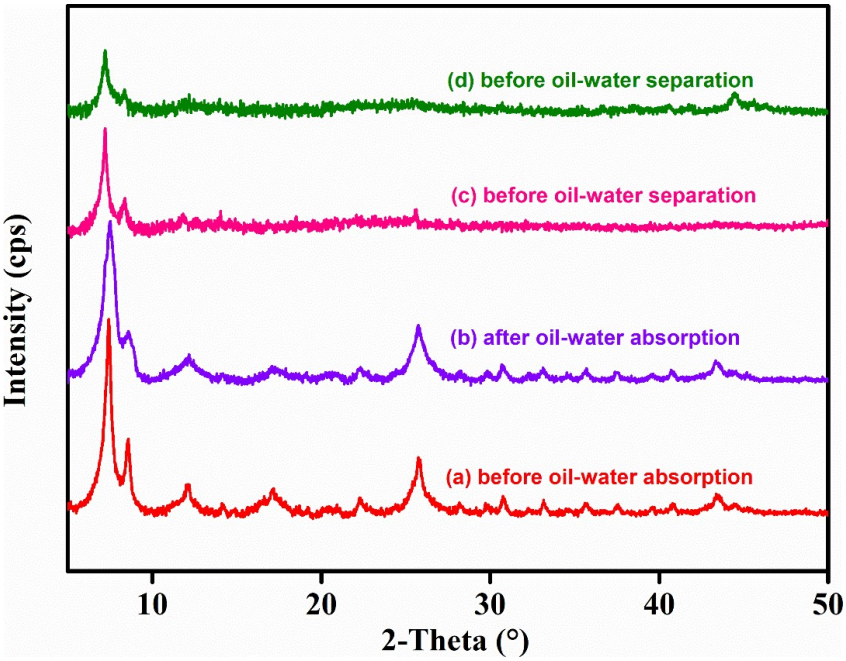

Fig. S36. PXRD patterns of **SH-UiO-66′@sponge** composite (a) before and (b) after oil absorption experiments and **SH-UiO-66′@silk** membrane (c) before and (d) after oil-water separation experiments.

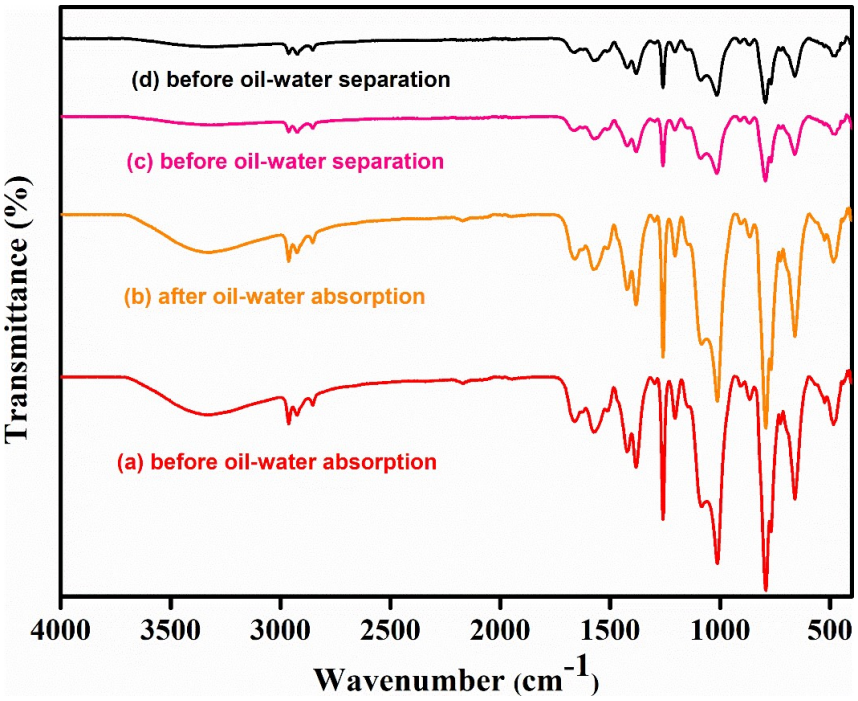

Fig. S37. ART-IR of **SH-UiO-66′@sponge** composite (a) before and (b) after oil absorption experiments and **SH-UiO-66′@silk** membrane (a) before and (d) after oil-water separation experiments.

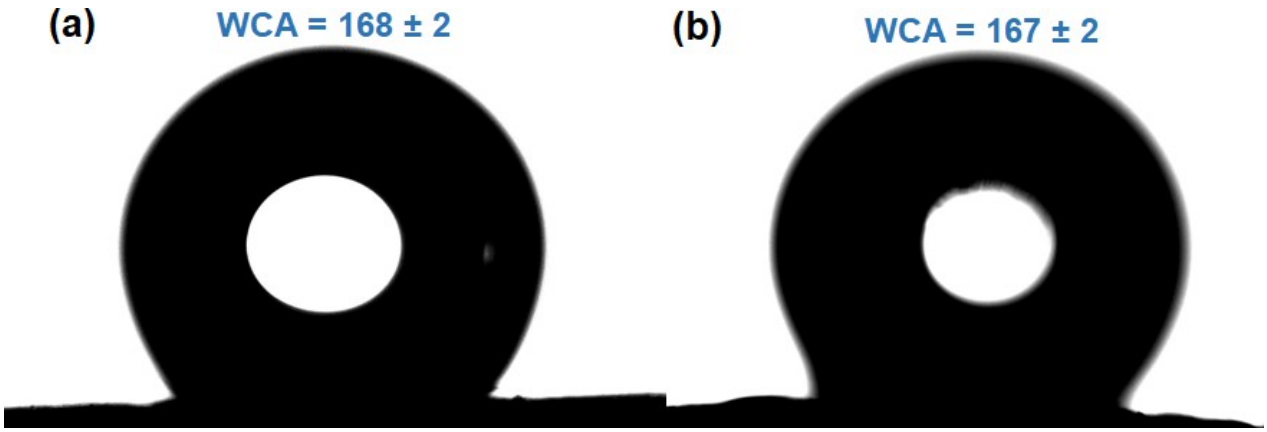

Fig. S38. WCA of **SH-UiO-66′@sponge** composite (a) after oil absorption experiments and **SH-UiO-66′@silk** membrane (b) after oil-water separation experiments.

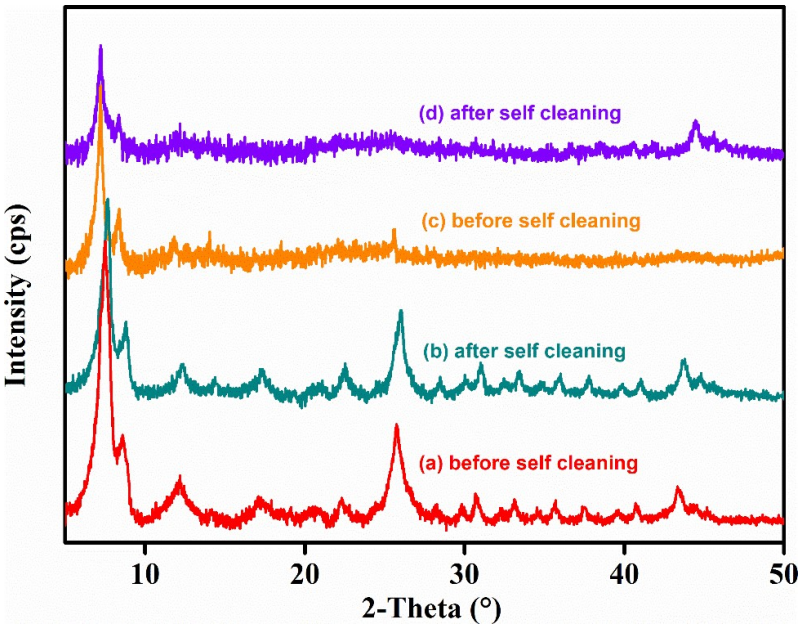

Fig. S39. PXRD patterns of **SH-UiO-66′@sponge** (a) before and (b) after self-cleaning and **SH-UiO-66′@silk** (c) before and (d) after self-cleaning.

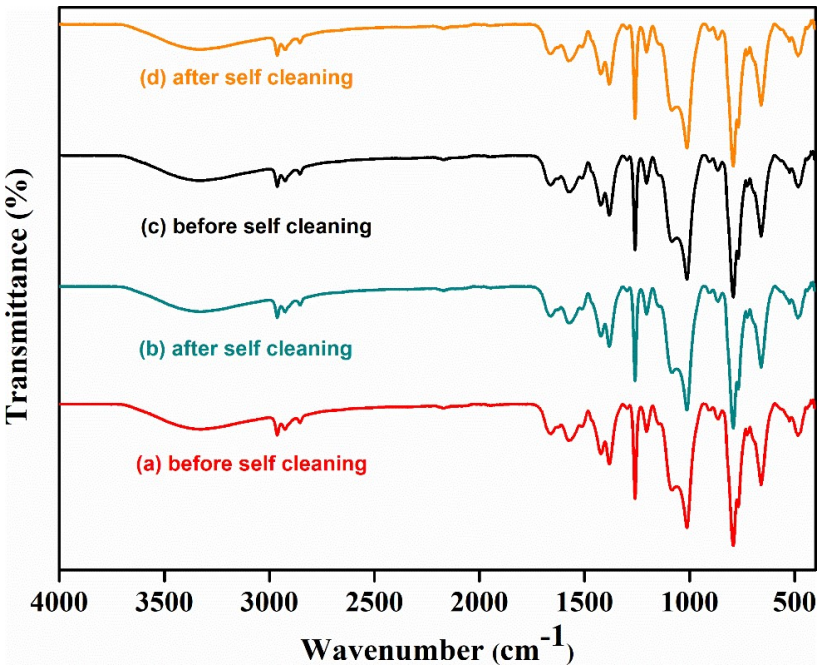

Fig. S40. ART-IR of **SH-UiO-66′@sponge** (a) before and (b) after self-cleaning and **SH-UiO-66′@silk** (c) before and (d) after self-cleaning.

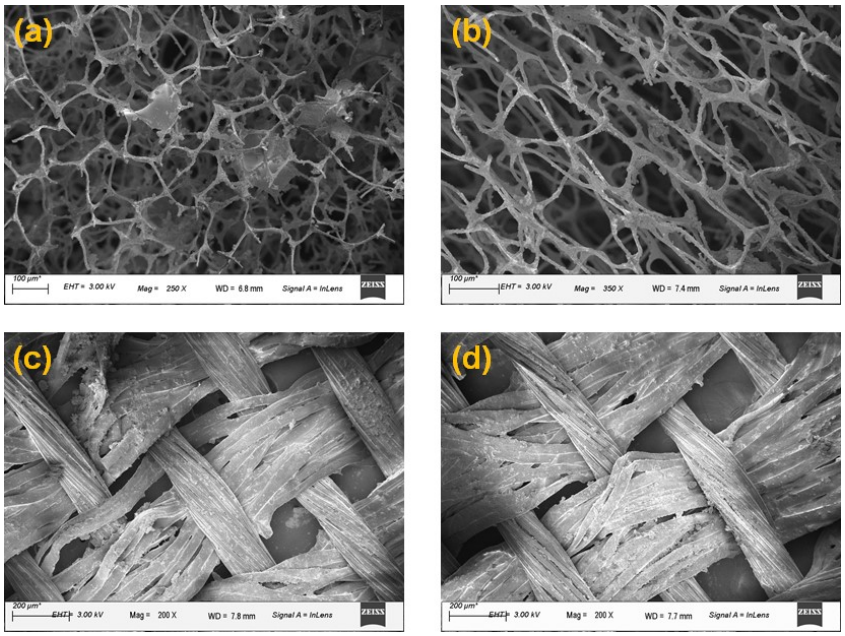

Fig. S41. High-resolution FE-SEM images of **SH-UiO-66′@sponge** (a) before and (b) after self-cleaning and **SH-UiO-66′@silk** (c) before and (d) after self-cleaning.

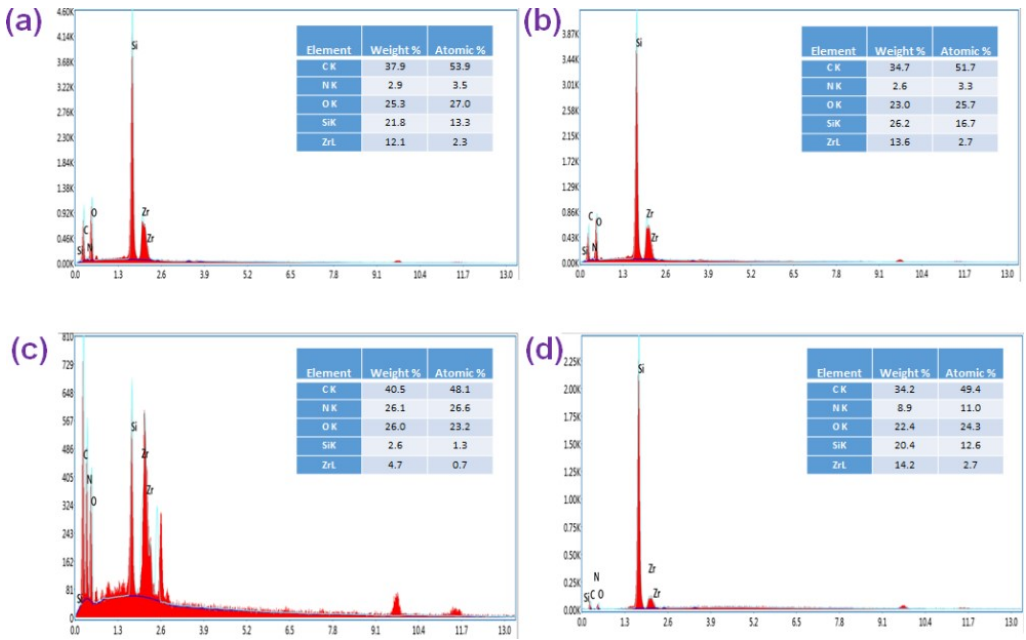

Fig. S42. EDX spectrum of **SH-UiO-66′@sponge** (a) before and (b) after self-cleaning and **SH-UiO-66′@silk** (c) before and (d) after self-cleaning.

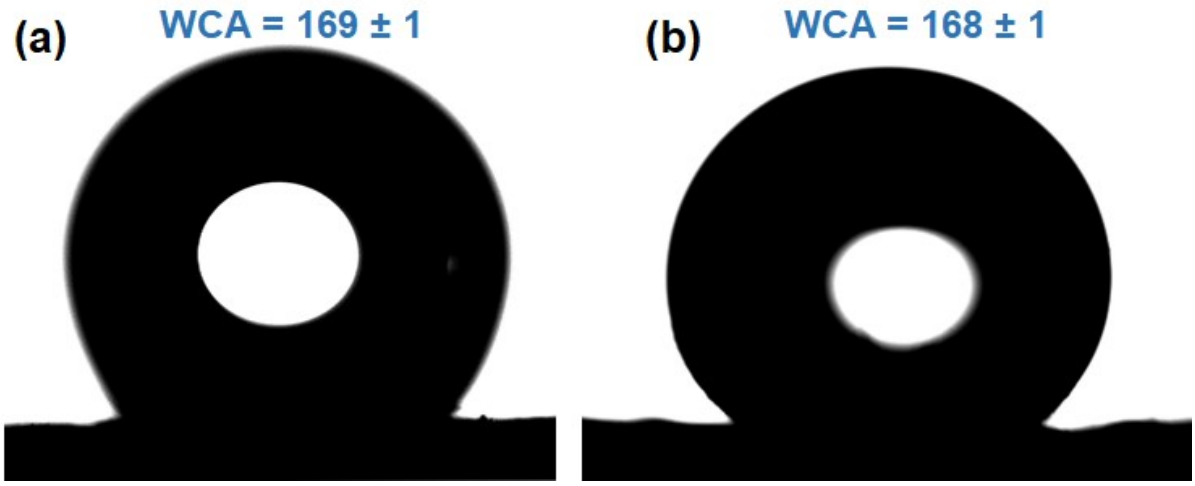

Fig. S43. WCA of **SH-UiO-66′@sponge** (a) after self-cleaning and **SH-UiO-66′@silk** (b) after self-cleaning.

Table S4. Comparison of important parameters of superhydrophobic absorbents or membranes materials for oil water separation.

S. No.	Absorbents	Absorption substances	Absorption capacity (g/g)	Oil-water separation efficiency (%)	Flux of Oil-water separation ($Lm^{-2}h^{-1}$)	Ref.
1	SH-UiO-66′@sponge and SH-UiO-	diesel oil, petrol oil, kerosene, crude oil, dichloromethane,	43.8-97.2	≥ 99	58263-47416	this work

	66′@membrane	chloroform, carbon tetrachloride, ethyl acetate, hexane, toluene				
2	PDMS-TiO_2-PU sponge	diesel oil, pump oil, silicone oil, edible oil, kerosene, dichloromethane, chloroform	16.7-43.5	NA	NA	1
3	SH-UiO-66@CFs	motor oil, silicone oil, gasoline, kerosene, toluene, hexane, ethyl acetate, carbon tetrachloride, chloroform, dichlomrthane	27.1-49.2	95-98	NA	2
4	superhydrophobic/superoleophilic sawdust	crude oil, n-hexane, gasoline, diesel oil, engine oil	10.0-17.5	NA	NA	3
5	cotton fiber modified via the sol-gel method	diesel oil, lubrication oil, crude oil, peanut oil	25.6-57.0	98.5	NA	4
6	modified jute fiber via the sol-gel method	crude oil, diesel oil, lubricatiom oil, peanut oil	7.4-10.2	NA	NA	5
7	mesoporous silica aerogel	petrol oil, diesel oil, toluene	19.1-18.6	NA	NA	6
8	ultralight cellulose-based aerogel	pump oil, diesel oil, chloroform, dodecane, hexane, soybean oil, pump oil, diseal oil, motor oil, heptane, tolune, DMSO, isopropanol	18.0-41.8	NA	NA	7
9	cellulose-based aerogel	crude oil, diesel oil, lubrication oil silicone oil, soyabean oil, toluene, n-hexane, trichloromethane, acetone, ethanol	60.4-152.3	NA	NA	8
10	polystyrene branched 9-octadecenoic acid grafted graphene	hexane, heptane, nonane, decane, hexadecane	11.0-27.0	NA	NA	9
11	MOF-PU sponge	n-hexane, paraffin, ethanol, edible oil, DMF, carbon	29.0-56.0	>96	NA	10

		tetrachloride				
12	UiO-66-F4@rGO/MS	n-hexane, isooctane, dichloromethane, 1,3,5-trimethylbenzene, silicone oil diesel oil light diesel oil crude oil	26.0-61.0	99.73	NA	11
13	MOF@Rgo composites	chloroform, n-hexane, silicone oil, bump oil, bean oil, toluene, acetone, butanone	14.0-37.0	>98	NA	12
14	MOFs-copper foam	soybean oil, n-hexane, isooctane, gasoline, dichloromethane, chloroform	1.5-3.5	>96	NA	13
15	FGO@MOG	crude oil, decane, heptane, hexane, octadecane, octane, petrolether, pentane, toluene, veg oil, carbon tetrachloride	2.0-5.0	NA	NA	14
16	Macroporous silicone sponges	crude oil, sunflower oil, kerosene, diesel, alcohol, acetic acid, chloroform, acetone, diethyl ether, n-hexane, isooctane, dichloromethane	9.7-27.0	>99	NA	15
17	GO/PDA coated fabric	formamide, engine oil, ethylene glycol, liquide paraffin, propylene carbonate, rapeseed oil	NA	>99.50	1452 - 308	16
18	CBM-CuO-SA	n-hexane, toluene, trichloromethane	NA	>96	141	17
19	PVDF membrane	water-in-petroleum ether, water-in-toluene, water-in-isooctane, and water-in-dichloromethane	NA	NA	NA	18
20	$Cu(OH)_2$@ZIF-8 membrane	heptane, cychlohexane, toluene, trichloromethane diesel, dichloromethane,	NA	>97	90 000	19

		petroleum				
21	UiO-66-NH-C18-PSM	Diesel, hexane, ethyl acetate, acetone, toluene, decane, dichloromethane	32.3 - 66.1	>99	NA	20
22	SMIL-101(Cr)-PSM	Petrol, chloroform, hexane, toluene	1.18-2.81	>99	NA	21
23	OctA/rGA composite	DCM, Chloroform, Toluene, Benzene, chloroform, dichloromethane, hexadecane, p-xylene, ethylbenzene	4.70-16.12	NA	Very less	22

References:

1. Shuai, Q.; Yang, X.; Luo, Y.; Tang, H.; Luo, X.; Tan, Y.; Ma, M., A superhydrophobic poly(dimethylsiloxane)-TiO2 coated polyurethane sponge for selective absorption of oil from water. *Mater. Chem. Phys.* **2015,** *162*, 94-99.
2. Dalapati, R.; Nandi, S.; Gogoi, C.; Shome, A.; Biswas, S., Metal-organic framework (MOF) derived recyclable, superhydrophobic composite of cotton fabrics for the facile removal of oil spills. *ACS Appl. Mater. Interfaces* **2021,** *13*, 8563-8573.
3. Zang, D.; Liu, F.; Zhang, M.; Gao, Z.; Wang, C., Novel superhydrophobic and superoleophilic sawdust as a selective oil sorbent for oil spill cleanup. *Chem. Eng. Res. Des.* **2015,** *102*, 34-41.
4. Lv, N.; Wang, X.; Peng, S.; Luo, L.; Zhou, R., Superhydrophobic/superoleophilic cotton-oil absorbent: preparation and its application in oil/ water separation. *RSC Adv.* **2018,** *8*, 30257-30264.
5. Lv, N.; Wang, X.; Peng, S.; Zhang, H.; Luo, L., Study of the kinetics and equilibrium of the adsorption of oils onto hydrophobic jute fiber modified via the sol-gel method. *Int. J. Environ. Res. Public Health* **2018,** *15*, 969.
6. Zhang, C.; Dai, C.; Zhang, H.; Peng, S.; Wei, X.; Hu, Y., Regeneration of mesoporous silica aerogel for hydrocarbon adsorption and recovery. *Mar. Pollut. Bull.* **2017,** *122*, 129-138.
7. Zhang, H.; Li, Y.; Xu, Y.; Lu, Z.; Chen, L.; Huang, L.; Fan, M., Versatile fabrication of a superhydrophobic and ultralight cellulose-based aerogel for oil spillage clean-up. *Phys. Chem. Chem. Phys.* **2016,** *18*, 28297-28306.
8. Yin, T.; Zhang, X.; Liu, X.; Wang, C., Resource recovery of Eichhornia crassipes as oil superabsorbent. *Mar. Pollut. Bull.* **2017,** *118*, 267-274.
9. Alghunaimi, F. I.; Alsaeed, D. J.; Harith, A. M.; Saleh, T. A., Synthesis of 9-octadecenoic acid grafted graphene modified with polystyrene for efficient light oil removal from water. *J. Clean. Prod.* **2019,** *233*, 946-953.
10. He, Z.; Wu, H.; Shi, Z.; Duan, X.; Ma, S.; Chen, J.; Kong, Z.; Chen, A.; Sun, Y.; Liu, X., Mussel-inspired durable superhydrophobic/superoleophilic MOF-PU sponge with high chemical stability, efficient oil/water separation and excellent anti-icing properties. *Colloids Surf. A Physicochem. Eng. Asp.* **2022,** *648*, 129142.
11. Zhan, Y.; He, S.; Hu, J.; Zhao, S.; Zeng, G.; Zhou, M.; Zhang, G.; Sengupta, A., Robust super-hydrophobic/super-oleophilic sandwich-like UIO-66-F4@rGO composites for efficient and multitasking oil/water separation applications. *J. Hazard. Mater.* **2020,** *388*, 121752.

12. Gu, J.; Fan, H.; Li, C.; Caro, J.; Meng, H., Robust superhydrophobic/superoleophilic wrinkled microspherical MOF@rGO compositesfor efficient oil-water separation. *Angew. Chem. Int. Ed.* **2019,** *58*, 5297-5301.
13. Du, J.; Zhang, C.; Pu, H.; Li, Y.; Jin, S.; Tan, L.; Zhou, C.; Dong, L., HKUST-1 MOFs decorated 3D copper foam with superhydrophobicity/superoleophilicity for durable oil/water separation. *Colloids Surf. A Physicochem. Eng. Asp.* **2019,** *573*, 222-229.
14. Jayaramulu, K.; Geyer, F.; Petr, M.; Zboril, R.; Vollmer, D.; Fische, R. A., Shape controlled hierarchical porous hydrophobic/oleophilic metal-organic nanofibrous gel composites for oil adsorption. *Adv. Mater.* **2017,** *29*, 1605307.
15. Cao, J.; Wang, D.; An, P.; Zhang, J.; Feng, S., Highly compression-tolerant and durably hydrophobic macroporous silicone sponges synthesized by a one-pot click reaction for rapid oil/water separation. *J. Mater. Chem. A* **2018,** *6*, 18025-18030.
16. Zhu, X.; Gao, Z.; Li, F.; Miao, G.; Xu, T.; Miao, X.; Song, Y.; Li, X.; Ren, G., Superlyophobic graphene oxide/polydopamine coating under liquid system for liquid/liquid separation, dye removal, and anti-corrosion. *Carbon* **2022,** *190*, 329-336.
17. Yin, Z.; Yuan, F.; Xue, M.; Xue, Y.; Xie, Y.; Ou, J.; Luo, Y.; Hong, Z.; Xie, C., A multifunctional and environmentally safe superhydrophobic membrane with superior oil/water separation, photocatalytic degradation and anti-biofouling performance. *J. Colloid Interface Sci.* **2022,** *611*, 93-104.
18. W.Zhang; Shi, Z.; Zhang, F.; Liu, X.; Jin, J.; Jiang, L., Superhydrophobic and superoleophilic PVDF membranes for effective separation of water-in-oil emulsions with high flux. *Adv. Mater.* **2013,** *25*, 2071-2076.
19. Li, Q.; Deng, W.; Li, C.; Sun, Q.; F.Huang; Zhao, Y.; Li, S., High-flux oil/water separation with interfacial capillary effect in switchable superwetting Cu(OH)2@ZIF-8 nanowire membranes. *ACS Appl. Mater. Interfaces* **2018,** *10*, 40265–40273.
20. Shi, M.; Huang, R.; Qi, W.; Su, R.; He, Z., Synthesis of superhydrophobic and high stable Zr-MOFs for oil-water separation. *Colloids Surf. A Physicochem. Eng.* **2020,** *602*, 125102.
21. Gao, M.; Zhao, S.; Chen, Z.; Liu, L.; Han, Z., Superhydrophobic/superoleophilic MOF composites for oil−water separation. *Inorg. Chem.* **2019,** *58*, 2261–2264.
22. Kang, D. W.; Kang, M.; Choe, J. H.; Kim, H.; Kim, D. W.; Hong, C. S., Fine-tuning of wettability in a single metal–organic framework via postcoordination modification and its reduced graphene oxide aerogel for oil–water separationS. Eom. *Chem. Sci.* **2019,** *10*, 2663-2669.